Observation of topological surface states of strained HgTe and their circular dichroism
Supplementary Material

Olivier Crauste,[1] Yoshiyuki Ohtsubo,[2] Philippe Ballet,[3] Pierre-André Delplace,[4] David Carpentier,[5] Clément Bouvier,[1] Tristan Meunier,[1] Amina Taleb,[2] and Laurent P. Lévy[1]

[1]*Institut Néel, C.N.R.S.- Université Joseph Fourier, BP 166, 38042 Grenoble Cedex 9, France*

[2]*Synchrotron SOLEIL, Saint-Aubin BP 48, F-91192 Gif-sur-Yvette, France*

[3]*CEA, LETI, MINATEC Campus, DOPT, 17 rue des martyrs 38054 Grenoble Cedex 9, France*

[4]*Département de Physique Théorique, Université de Genève, CH-1211 Genève 4, Switzerland*

[5]*Laboratoire de Physique, Ecole Normale Supérieure de Lyon and CNRS UMR5672, France*

(Dated: July 5, 2013)

EFFECT OF THE INCIDENT PHOTON ENERGY

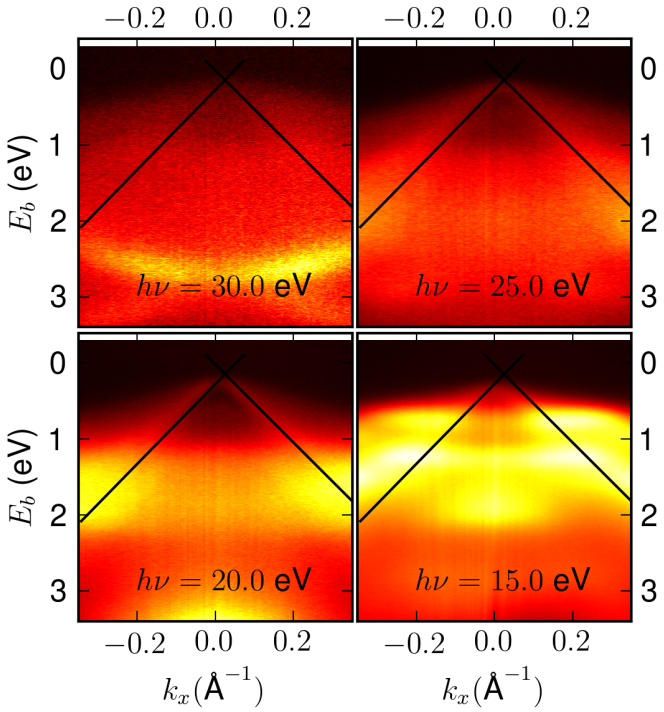

FIG. 1. The same sample is analyzed with incident photon energies $h\nu$ from 15 eV to 30 eV. The cone structure, emphasized with the black lines, stays unchanged whereas the bulk component of the spectra evolves with $h\nu$. This proves that the cone structure is a surface structure.

Varying the incident photon energy $h\nu$, shifts the binding energy of bulk bands according to the k_z dispersion. Since there is no k_z dispersion for surface states, no binding-energy shift is present. This is a powerful mechanism allowing to distinguish 2D states by changing photon energies.[1, 2] We can deduce from the evolution on the ARPES spectra with a varying incident energy what structure can be attributed to surface of the sample and what comes from the bulk. The former shows no evolution with the photon energy as the latter does. The spectra presented on the figure 1 were obtained for photon energy varying from 15 eV to 30 eV. The black straight lines has the same dispersion relation as used in the present paper. On each of spectra, the cone structure remains identical, whereas the other structures seen on these spectra evolves with the photon energy. This is a strong indication that this cone structure comes from surface states.

ARPES SPECTRUM FROM THE Γ TO X POINT

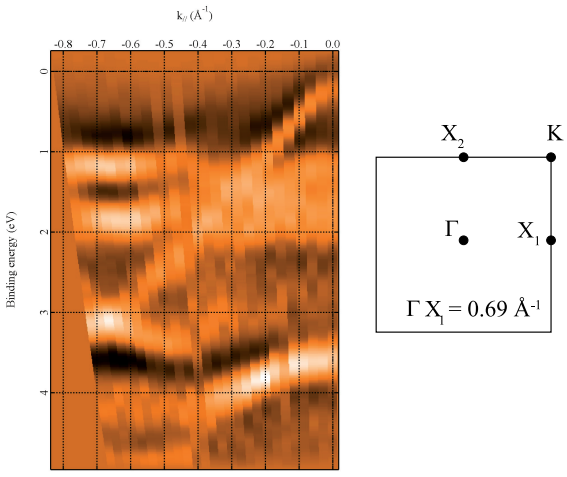

FIG. 2. Left: Γ to $X1$ ARPES spectrum. The Dirac spectrum observed close to the Γ-point extends all the way to the X point with the same linear slope. Right: symmetry points of the Surface Brillouin zone.

In addition to the high-resolution spectrum, we present the Γ to $X1$ spectrum obtained with the same undoped sample. The Dirac spectrum observed in the vicinity of the Γ point and confirmed theoretically is also observed here. This surface states spectrum remains surprisingly linear up to the X point of the Brillouin zone. The ARPES spectrum observed on a sample capped by a thin CdTe layer is quite similar: this confirms the robustness of this observation.

NUMERICAL SOLUTION OF THE KANE MODEL AT AN INTERFACE

8 bands Kane model

The low energy states of both HgTe and CdTe are accurately described by a Kane model involving 8 bands around the Γ point. The basis of states we consider is :

$$u_1(r) = |\Gamma_6, +1/2\rangle; u_2(r) = |\Gamma_6, -1/2\rangle \tag{1}$$

$$u_3(r) = |\Gamma_8, +3/2\rangle; u_4(r) = |\Gamma_8, +1/2\rangle; u_5(r) = |\Gamma_8, -1/2\rangle; u_6(r) = |\Gamma_8, -3/2\rangle \tag{2}$$

$$u_7(r) = |\Gamma_7, +1/2\rangle; u_8(r) = |\Gamma_7, -1/2\rangle. \tag{3}$$

We follow Novik et al. [3] and write the reduced Kane hamiltonian as

$$H^0 = \begin{pmatrix} T & 0 & -\sqrt{\frac{1}{2}}Pk_+ & \sqrt{\frac{2}{3}}Pk_z & \sqrt{\frac{1}{6}}Pk_- & 0 & -\sqrt{\frac{1}{3}}Pk_z & -\sqrt{\frac{1}{3}}Pk_- \\ 0 & T & 0 & -\sqrt{\frac{1}{6}}Pk_+ & \sqrt{\frac{2}{3}}Pk_z & \sqrt{\frac{1}{2}}Pk- & -\sqrt{\frac{1}{3}}Pk_+ & \sqrt{\frac{1}{3}}Pk_z \\ -\sqrt{\frac{1}{2}}k_-P & 0 & U+V & -\overline{S}_- & R & 0 & \sqrt{\frac{1}{2}}\overline{S}_- & -\sqrt{2}R \\ \sqrt{\frac{2}{3}}k_zP & -\sqrt{\frac{1}{6}}k_-P & -\overline{S}_-^\dagger & U-V & C & R & \sqrt{2}V & -\sqrt{\frac{3}{2}}\tilde{S}_- \\ \sqrt{\frac{1}{6}}k_+P & \sqrt{\frac{2}{3}}k_zP & R^\dagger & C^\dagger & U-V & \overline{S}_+^\dagger & -\sqrt{\frac{2}{3}}\tilde{S}_+ & -\sqrt{2}V \\ 0 & \sqrt{\frac{1}{2}}k_+P & 0 & R^\dagger & \overline{S}_+ & U+V & \sqrt{2}R^\dagger & \sqrt{\frac{1}{2}}\overline{S}_+ \\ -\sqrt{\frac{1}{3}}k_zP & -\sqrt{\frac{1}{3}}k_-P & \sqrt{\frac{1}{2}}\overline{S}^\dagger & \sqrt{2}V & -\sqrt{\frac{3}{2}}\tilde{S}_+^\dagger & \sqrt{2}R & U-\Delta & C \\ -\sqrt{\frac{1}{3}}k_+P & -\sqrt{\frac{1}{3}}kz-P & -\sqrt{2}R^\dagger & -\sqrt{\frac{3}{2}}\tilde{S}_-^\dagger & -\sqrt{2}V & \sqrt{\frac{1}{2}}\overline{S}_+^\dagger & C^\dagger & U-\Delta \end{pmatrix}, \tag{4}$$

where

$$T = E_c(z) + \frac{\hbar^2}{2m_0}\left((2F+1)k_\parallel^2 + k_z(2F+1)k_z\right) \tag{5a}$$

$$U = E_v(z) - \frac{\hbar^2}{2m_0}\left(\gamma_1 k_\parallel^2 + k_z\gamma_1 k_z\right) \tag{5b}$$

$$V = -\frac{\hbar^2}{2m_0}\left(\gamma_2 k_\parallel^2 - 2k_z\gamma_2 k_z\right) \tag{5c}$$

$$R = -\frac{\hbar^2}{2m_0}\sqrt{3}\left(\mu k_+^2 - \overline{\gamma}k_-^2\right) \tag{5d}$$

$$\overline{S}_\pm = -\frac{\hbar^2}{2m_0}\sqrt{3}k_\pm\left(\{\gamma_3, k_z\} + [\kappa, k_z]\right) \tag{5e}$$

$$\tilde{S}_\pm = -\frac{\hbar^2}{2m_0}\sqrt{3}k_\pm\left(\{\gamma_3, k_z\} - \frac{1}{3}[\kappa, k_z]\right) \tag{5f}$$

$$C = \frac{\hbar^2}{m_0}k_-[\kappa, k_z]. \tag{5g}$$

The parameters for the different materials considered are listed in the following table.

	E_c	E_v	$E_P = 2m_0P^2/\hbar^2$	F	γ_1	$\gamma 2$	γ_3	κ
HgTe	-0.303 eV	0 eV	18.8 eV	0	4.1	0.5	1.3	-0.4
CdTe	1.03 eV	-0.57 eV	18.8 eV	-0.09	1.47	-0.28	0.03	-1.31
Vacuum	$\simeq$+5 eV	$\simeq$-10eV	0	0	0	0	0	0

Similarly, the bulk strain induced by the mismatch of lattice spacing with CdTe is incor-

porated through a Bir-Pikus Hamiltonian

$$H_{BP} = \begin{pmatrix} T_{BP} & 0 & 0 & 0 & 0 & 0 & 0 & 0 \\ 0 & T_{BP} & 0 & 0 & 0 & 0 & 0 & 0 \\ 0 & 0 & U_{BP}+V_{BP} & -S^-_{BP} & R_{BP} & 0 & \sqrt{\frac{1}{2}}S^-_{BP} & -\sqrt{2}R_{BP} \\ 0 & 0 & -S^+_{BP} & U_{BP}-V_{BP} & 0 & R_{BP} & \sqrt{2}V_{BP} & -\sqrt{\frac{3}{2}}S^-_{BP} \\ 0 & 0 & R^\dagger_{BP} & 0 & U_{BP}-V_{BP} & (S^+_{BP})^\dagger & -\sqrt{\frac{2}{3}}S^+_{BP} & -\sqrt{2}V_{BP} \\ 0 & 0 & 0 & R^\dagger_{BP} & S^+_{BP} & U_{BP}+V_{BP} & \sqrt{2}R^*_{BP} & \sqrt{\frac{1}{2}}S^+_{BP} \\ -0 & 0 & \sqrt{\frac{1}{2}}(S^-_{BP})^\dagger & \sqrt{2}V_{BP} & -\sqrt{\frac{3}{2}}(S^+_{BP})^\dagger & \sqrt{2}R_{BP} & U_{BP}-\Delta_{BP} & 0 \\ 0 & 0 & -\sqrt{2}R^\dagger_{BP} & -\sqrt{\frac{3}{2}}\tilde{S}^\dagger_- & -\sqrt{2}V & \sqrt{\frac{1}{2}}\overline{S}^\dagger_+ & 0 & U-\Delta \end{pmatrix} \tag{6}$$

with

$$T_{BP} = \frac{\hbar^2}{2m_0}(2F+1)\left(\epsilon_{xx}+\epsilon_{yy}+\epsilon_{zz}\right) \tag{7a}$$

$$U_{BP} = -\frac{\hbar^2}{2m_0}\gamma_1\left(\epsilon_{xx}+\epsilon_{yy}+\epsilon_{zz}\right) \tag{7b}$$

$$V_{BP} = -\frac{\hbar^2}{2m_0}\gamma_2\left(\epsilon_{xx}+\epsilon_{yy}-2\epsilon_{zz}\right) \tag{7c}$$

$$R_{BP} = -\frac{\hbar^2}{2m_0}\sqrt{3}\left(\gamma_2(\epsilon_{yy}-\epsilon_{xx})+2i\gamma_3\epsilon_{xy}\right) \tag{7d}$$

$$S^\pm_{BP} = -\frac{\hbar^2}{2m_0}\sqrt{3}\gamma_3 2(\epsilon_{xz}\pm\epsilon_{yz}), \tag{7e}$$

where the ϵ_{ij} are the component of the induced strain tensor.

Discrete model at the interface

We consider an interface between *e.g.* HgTe and CdTe (or vacuum) in the z direction. As the sample directions in the x and y directions are expected to be much larger than in the z direction, we need to discretize the Hamiltonian (4) only in the z direction. We consider an system infinite or large enough in (x, y) directions so that k_x and k_y remain good quantum numbers. In the z direction orthogonal to the interface, the hamiltonian is discretized through the following standard procedure :

$$k_z f(z) \to -\frac{i}{2a}(f_{n+1}-f_{n-1}). \tag{8}$$

Special care is devoted to the off-diagonal linear in k_z terms, to ensure the hermiticity of the discrete hamiltonian. We introduce an ad-hoc lattice constant a which can be freely adjusted

: the motivation to do so is to enforce an independence of our result on the discretization scheme in a given range of energy and momentum. In particular, the discretization introduce higher k terms in the hamiltonian, which are a dependent, and should be kept irrelevant in the range of parameters considered. Moreover, while the Kane model is valid only at small k, the interface is expected to occur on a few nanometers : a varying discretization parameter a allows to study the dependance of our results on the sharpness of the interface.

We choose periodic boundary conditions in the z direction for the surrounding materials (CdTe or vacuum), and introduce two smooth interfaces at $z = 0$ and $z = L$ with HgTe present for $0 < z < L$. The interfaces are described by a smooth function $\phi(z/\xi)$ which extrapolate the Kane parameters between the values of both materials. The extrapolating function $\phi(z/\xi)$ is parametrized by a length ξ which accounts for the smoothness of the interface. We have checked an independence of our results on this sharpness. The corresponding z dependent Schrödinger equation is then solved numerically.

---

[1] A. Damascelli, Physica Scripta **T109**, 61 (2004).

[2] A. L. Wachs, T. Miller, T. C. Hsieh, A. P. Shapiro, and T. C. Chiang, Physical Review B **32**, 2326 (1985).

[3] E. Novik, A. Pfeuffer-Jeschke, T. Jungwirth, V. Latussek, C. Becker, G. Landwehr, H. Buhmann, and L. Molenkamp, Physical Review B **72** (2005).